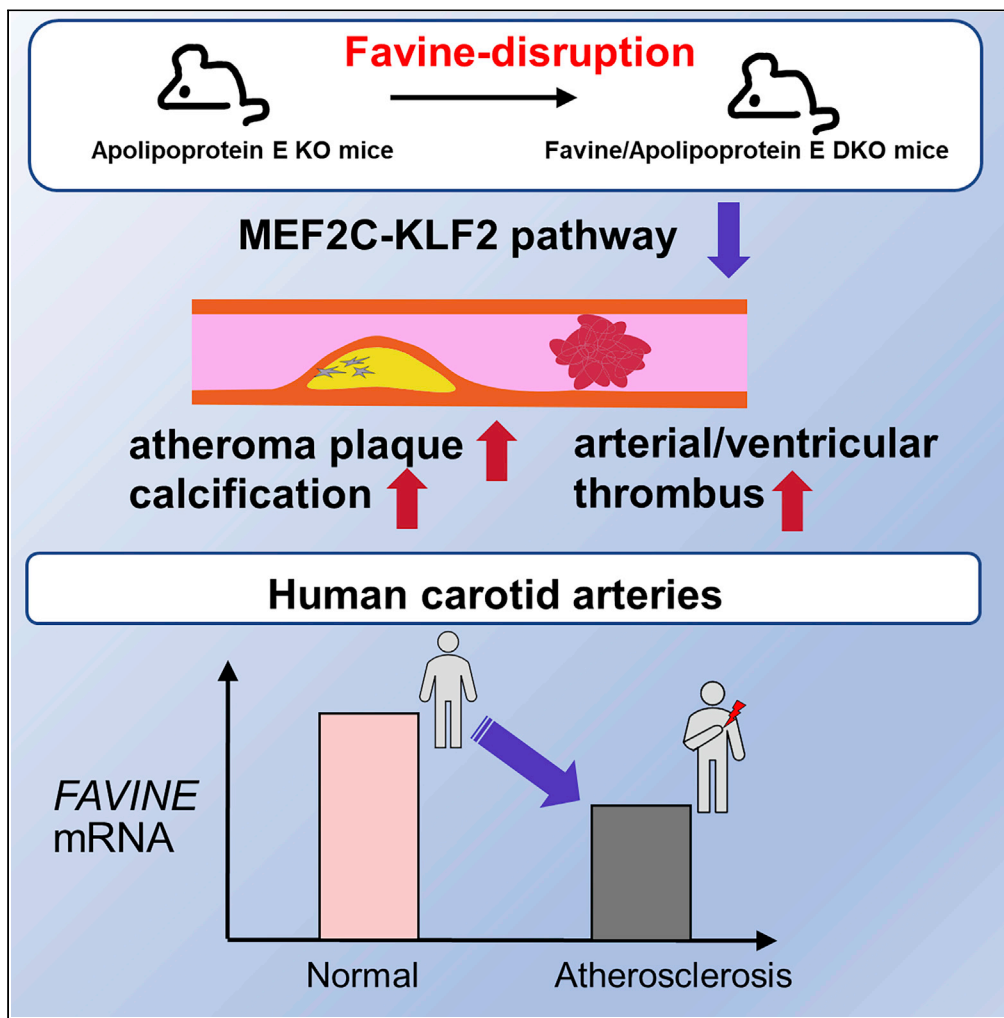


Article

Favine/CCDC3 deficiency accelerated atherosclerosis and thrombus formation is associated with decreased MEF2C-KLF2 pathway



Sachiko Kobayashi, Shunbun Kita, Daisuke Okuzaki, ..., Atsunori Fukuhara, Eiichi Morii, Ichihiro Shimomura

skobayashi@endmet.med.osaka-u.ac.jp (S.K.)
shunkita@endmet.med.osaka-u.ac.jp (S.K.)

Highlights

Favine deficiency in apoE KO mice accelerated atherosclerosis and thrombosis

The atherosclerotic lesions were accompanied by cholesterol crystals and calcification

Human *FAVINE* mRNA expressions decreased with the progression of atherosclerosis

Favine deficiency was associated with a decreased MEF2C-KLF2 pathway

Kobayashi et al., iScience 25, 105252
November 18, 2022 © 2022 The Authors.
<https://doi.org/10.1016/j.isci.2022.105252>



Article

Favine/CCDC3 deficiency accelerated atherosclerosis and thrombus formation is associated with decreased MEF2C-KLF2 pathway

Sachiko Kobayashi,^{1,10,*} Shunbun Kita,^{1,2,*} Daisuke Okuzaki,³ Yuya Fujishima,¹ Michio Otsuki,^{1,4} Hisashi Kato,⁵ Yasuko Nishizawa,⁶ Kazuya Miyashita,⁷ Chieko Yokoyama,^{1,8} Atsunori Fukuhara,^{1,2} Eiichi Morii,⁹ and Ichihiro Shimomura¹

SUMMARY

Currently, no mouse models manifest calcification and thrombus formation, which is frequently associated with human atherosclerosis. We demonstrated that lack of Favine/CCDC3 in apoE knockout mice accelerated atherosclerosis accompanied by large cholesterol crystals and calcification, and also promoted thrombus formation in the left ventricle and arteries. Circulating Favine was detectable in WT mouse plasma. RNA-sequencing analysis of aortae in DKO mice showed similar gene expression patterns of human atherosclerosis with unstable and vulnerable plaques. Importantly, human *FAVINE* mRNA expressions were lower in atheroma plaque than in adjacent intact aortic tissue and decreased with the progression of atherosclerosis. Pathway analysis of aortae in DKO mice suggested the decrease of the MEF2C-KLF2-mediated transcriptional pathway. Favine insufficiency and its attenuated downstream pathways may increase atherosclerosis progression with calcification and thrombus, which have not previously been fully modeled in experimental animals. Favine and its downstream pathways may have therapeutic potential for atherosclerosis.

INTRODUCTION

Human advanced atherosclerotic lesions are accompanied by calcifications, necrotic cores with deposited cholesterol crystals, and subsequent thrombus formation. (Eckel et al., 2021). Vascular calcification is a characteristic feature of advanced atherosclerosis and is predictive of cardiovascular events (Doherty et al., 2003; Nicoll and Henein, 2014; Rattazzi et al., 2005). Despite its clinical importance, the molecular mechanisms involved in the regulation of vascular calcification are not fully clear, in part because murine atherogenic models with calcification are unavailable (Yahagi et al., 2017).

Previously, we identified fat/vessel-derived secretory protein/coiled-coil domain-containing 3/(Favine/CCDC3) (Kobayashi et al., 2010). *FAVINE* mRNA is abundantly expressed in human arteries, including the aorta, coronary artery, and tibial artery (Figure S1, data obtained from GTEX Portal). We showed that Favine has adipogenic and lipogenic functions in 3T3-L1 adipocytes and mice (Kobayashi et al., 2015). However, the function of Favine in atherosclerosis has not been previously addressed.

Here, we demonstrated that Favine deficiency exacerbated ApoE-deficient mice from human-like advanced atherosclerosis lesion formation accompanied by cholesterol crystals, calcification, and thrombosis. Favine deficiency was associated with decreased MEF2C-KLF2 pathway.

RESULTS

Generation of combined ApoE and favine deficient mice

To investigate the function of Favine in atherosclerosis, we generated Favine/ApoE double KO mice. Favine-deficient mice (Kobayashi et al., 2015) were bred with ApoE-deficient mice (Plump et al., 1992) to generate single (ApoE $-/-$, Favine $-/-$) and combined (ApoE $-/-$ /Favine $-/-$) deficiencies in ApoE and Favine. All mice appeared normal at birth and displayed normal neonatal weight gain and survival, regardless of genotype. The body weight was similar between the two genotype groups (Table 1).

¹Department of Metabolic Medicine, Graduate School of Medicine, Osaka University, 2-2 Yamadaoka, Suita, Osaka 565-0871, Japan

²Department of Adipose Management, Graduate School of Medicine, Osaka University, 2-2 Yamadaoka, Suita, Osaka 565-0871, Japan

³Immunology Frontier Research Center, Osaka University, 3-1 Yamadaoka, Suita, Osaka 565-0871, Japan

⁴Department of Endocrinology, Graduate School of Medical Science, Tokyo Women's Medical University, Kawada-cho, Shinjuku-ku, Tokyo 162-8666 Tokyo, Japan

⁵Department of Hematology and Oncology, Graduate School of Medicine, Osaka University, 2-2 Yamadaoka, Suita, Osaka 565-0871, Japan

⁶Research Institute, Nozaki Tokushukai Hospital, 2-10-50 Tanigawa, Daitou, Osaka 574-0074, Japan

⁷Immuno-Biological Laboratories Co., Ltd., 1091-1 Naka, Fujioka, Gunma 375-0005, Japan

⁸Department of Nutrition and Life Science, Kanagawa Institute of Technology, 1030 Shimoogino, Atsugi, Kanagawa 243-0292, Japan

⁹Department of Pathology, Graduate School of Medicine, Osaka University, 2-2 Yamadaoka, Suita, Osaka 565-0871, Japan

¹⁰Lead contact

*Correspondence: skobayashi@endmet.med.osaka-u.ac.jp (S.K.), shunkita@endmet.med.osaka-u.ac.jp (S.K.)

<https://doi.org/10.1016/j.isci.2022.105252>



Table 1. Characteristics of DKO mice

Body Weight (g)		ApoE KO	DKO	p-value
Normal chow	Young	20.7 ± 0.6	20.6 ± 0.6	n.s.
	Aged	28.0 ± 1.63	27.2 ± 1.45	n.s.
Western diet		32.5 ± 1.01	32.6 ± 1.25	n.s.

ApoE mice and DKO mice were fed either normal chow or a Western diet. Normal chow-fed mice were used at the age of 6 weeks or at the age of 1 year ($n = 6\sim 7$ for ApoE KO and $n = 6\sim 9$ for DKO mice). Western diet-fed mice were fed the diet for 4 months ($n = 13$ for ApoE KO and $n = 8$ for DKO mice). The body weight was measured. Data are mean ± SEM. Differences between the two groups were examined for statistical significance using Student's *t*-test. n.s., not significant.

Favine deficiency accelerated atherosclerosis

To evaluate the impact of Favine deficiency on the development and progression of atherosclerosis, ApoE^{-/-} (ApoE KO) mice and ApoE^{-/-} Favine^{-/-} (DKO) mice were maintained on a Western diet for 3 or 4 months or on normal chow up to the age of 12 months. We harvested the aortae from ApoE KO mice and DKO mice, and the gross appearance of the lesions was examined using *en face* Oil red O stain (Figures 1A and S2). Favine deficiency in ApoE KO mice increased atherosclerotic lesion formation. A larger amount of lipid core stained with Oil Red O was detected in DKO mice after 4 months on the Western diet (Figure 1B). Cholesterol clefts as a hallmark of advanced atherosclerotic plaques were found in the DKO mice (Figure 1C, arrow, Figure 1D). Aortae from ApoE^{+/+} Favine^{-/-} KO mice after 4 months of Western diet feeding were intact without atherosclerotic plaques (Figure S3). Intimal calcification is common in actual human atherosclerosis but is rarely observed in mouse models (Yahagi et al., 2017). In von Kossa calcium stain, specific staining of calcified tissue, black staining was readily detected in DKO mice, whereas ApoE KO mice scarcely had a well-identified calcified lesion (DKO mice 4/5 vs ApoE KO mice 1/6) (Figures 1E and 1F). Because of the rarity of arterial calcification in atherosclerosis-prone mice, including ApoE KO mice (Yahagi et al., 2017), it was noteworthy that the DKO mice frequently exhibited calcification. Neither hypercalcemia nor hyperphosphatemia explained the cause of the calcification in DKO mice because the serum levels of calcium and phosphate did not change between the genotypes (Table 2). The levels of plasma glucose, insulin, total cholesterol, and triglycerides were similar between the two genotypes (Table 2). These data suggested that exaggerated atherosclerosis and calcification in the DKO mice were independent of well-known atherosclerosis-promoting factors such as the severity of hyperglycemia, hyperinsulinemia, and dyslipidemia.

Favine deficiency caused spontaneous thrombosis

Strikingly, Western diet-fed DKO mice had left ventricular thrombus (Figure 2A) (2/5 in DKO mice vs 0/6 in ApoE KO). The heart tissue section contained an organized thrombus (Figure 2B).

To determine the contribution of Favine to the injured vasculature *in vivo*, we challenged ApoE KO and Favine/ApoE DKO mice with carotid artery ligation. Carotid artery occlusion typically results in inflammatory vessel changes, shrinkage, neointima formation, and narrowing of the vascular lumen (Mukai et al., 2006). ApoE-KO mice showed no neointima formation in the right common carotid artery after sham surgery (Figure 2C left). In contrast, blood flow cessation caused by ligation at the left common carotid artery led to increased neointima formation in all ApoE-KO mice (Figure 2C middle). Interestingly, increased neointima formation was found in some Favine/ApoE KO mice to different extents, and a large thrombus at the proximal portion of the ligated site was observed in Favine/ApoE DKO mice (Figure 2C right) (4/4 in DKO mice vs 0/5 in ApoE KO mice). These observations suggested that Favine deficiency accelerated spontaneous thrombus formation in ApoE-deficient mice.

Favine deficiency did not alter the expression levels of inflammatory genes

Atherosclerosis is an inflammatory condition associated with the infiltration of monocytes and other immune cells (Wolf and Ley, 2019). Next, we evaluated the degree of inflammation and macrophage infiltration in the aortae of DKO mice by gene expression analyses. As shown in Figure S4, the expression levels of several inflammatory molecules (*Vcam-1*, *Mcp-1*, and *Tnfa*) and macrophage markers (*Cd68*) were

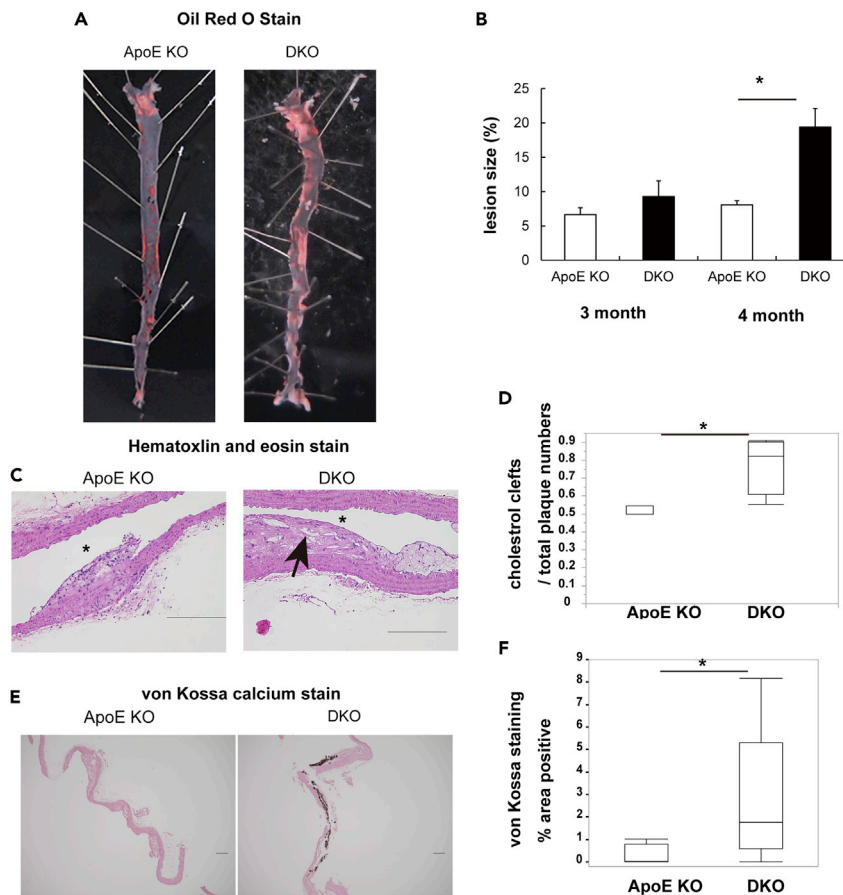


Figure 1. Favine deficiency augmented atherosclerosis and aortic intimal calcification

(A) Representative images of *En face* Oil red-O stain of the aorta from ApoE KO and Favine/ApoE DKO mice fed a Western diet for 4 months.

(B) Ratios of Oil red O-positive lesion areas to the total aortic wall areas. Data are mean \pm SEM ($n = 3$ for ApoE KO mice; $n = 4$ for DKO mice) * $p < 0.05$ versus ApoE KO mice by the Student's *t*-test.

(C) Representative hematoxylin and eosin (HE) stains of the aorta from ApoE KO and Favine/ApoE DKO mice fed a normal diet for 1 year. Asterisks indicate the lipid core. The arrows indicate cholesterol crystals. Scale bars are 200 μ m.

(D) Quantification of the number of cholesterol clefts normalized to total plaque numbers. In these box-and-whisker plots, lines within the boxes represent median values; the upper and lower lines of the boxes represent the 25th and 75th percentiles, respectively; and the upper and lower bars outside the boxes represent the 90th and 10th percentiles, respectively. * $p < 0.05$ versus ApoE KO mice by a Mann-Whitney *U* test ($n = 3$ for ApoE KO mice; $n = 4$ for DKO mice).

(E) Representative images of aortic sections with von Kossa calcium stain (black color). The aorta of DKO mice and the ApoE KO mice were fed the Western diet for 8 months. Scale bars are 200 μ m.

(F) Ratios of calcified region areas. In these box-and-whisker plots, lines within the boxes represent median values; the upper and lower lines of the boxes represent the 25th and 75th percentiles, respectively; and the upper and lower bars outside the boxes represent the 90th and 10th percentiles, respectively. * $p < 0.05$ versus ApoE KO mice by a Mann-Whitney *U* test ($n = 6$ for ApoE KO mice; $n = 5$ for DKO mice). See also [Figures S1–S3](#).

unchanged between the genotypes. Favine deficiency did not alter the mRNA level of *Nos3*, which is an important enzyme involved in the control of vascular homeostasis.

RNA-Seq analysis identified the molecular signature of atherosclerosis, arterial calcification, and thrombosis

To investigate the mechanisms of atherosclerosis progression, calcification, and thrombosis in DKO mice, bulk RNA-seq analysis of the aortas of ApoE KO mice and DKO mice fed normal chow for 1

Table 2. Plasma parameters of DKO mice

	Normal chow			Western diet		
	ApoE KO	DKO	p-value	ApoE KO	DKO	p-value
Blood glucose (mg/dL)	161.9 ± 17.2	161.2 ± 11.7	n.s.	202.1 ± 13.9	171.8 ± 16.5	n.s.
Insulin (ng/μL)	0.44 ± 0.09	0.62 ± 0.08	n.s.	2.07 ± 0.55	1.14 ± 0.31	n.s.
Total cholesterol (mg/dL)	369.5 ± 47.2	413 ± 33.8	n.s.	960.0 ± 53.3	872.4 ± 87.3	n.s.
Triglyceride (mg/dL)	289.8 ± 35.5	371.5 ± 44.3	n.s.	294.4 ± 41.8	242.0 ± 42.3	n.s.
Plasma PAI-1 (ng/mL)	6.0 ± 0.4	6.0 ± 0.7	n.s.	9.3 ± 1.0	8.4 ± 0.4	n.s.
Calcium (mg/dL)	n.d.	n.d.	n.s.	8.2 ± 0.37	8.0 ± 0.4	n.s.
Phosphate (mg/dL)	n.d.	n.d.	n.s.	8.0 ± 0.8	6.7 ± 0.9	n.s.

ApoE mice and DKO mice were fed normal chow for 1 year ($n = 4$ for ApoE KO and $n = 3$ for DKO mice) or a Western diet for 4 months ($n = 13$ for ApoE KO and $n = 10$ for DKO mice).

Plasma parameters were measured under ad-lib. Data are mean ± SEM. n.d., not determined. Differences between the two groups were examined for statistical significance using Student's *t*-test. n.s., not significant. See also [Figure S9](#) and [Table S4](#).

year was carried out. It has been reported that there are many differentially expressed genes between the aortae of two different murine strains when fed normal chow than when fed a Western diet (Yuan et al., 2009). With reference to this report, bulk RNA-seq analysis of aortae from ApoE KO mice and DKO mice fed normal chow was carried out, and 14612 genes were identified after we filtered low-expression genes (FPKM < 0.1). Then, we focused on 228 significant differentially expressed genes (p -value < 0.05 and Fold change ≥ 1.5). Among them, 133 were downregulated and 95 were upregulated (Figure 3A). The significant differentially expressed genes (DEGs) were annotated using ingenuity pathway analysis (IPA). The top 10 downregulated DEGs (Figure 3B and Table S1) and the top 10 upregulated DEGs (Figure 3C and Table S2) were listed. We used the z-score and p -value to identify the most important downstream effects of the 228 DEGs (Kramer et al., 2014). A positive z-score indicates increased functional activity in DKO mice relative to ApoE KO mice. Favine deficiency was associated with the 10 main functions related to several cellular processes (Figure 3D), as judged by the p -values

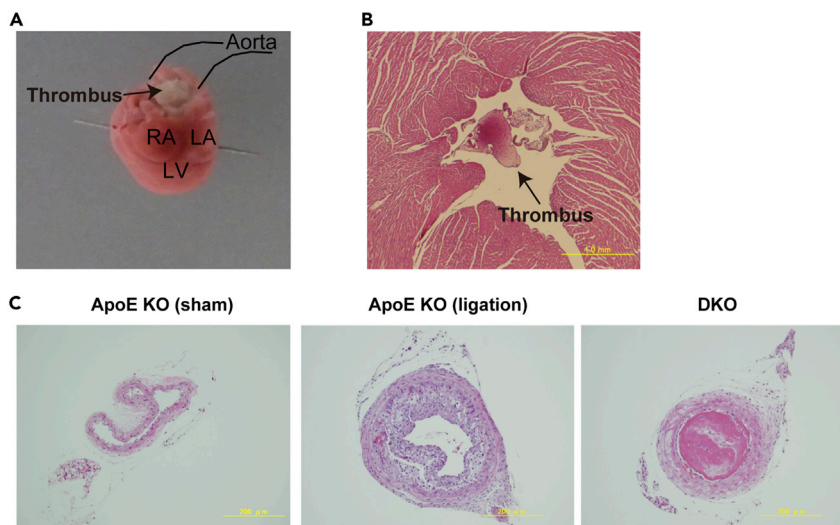


Figure 2. Favine deficiency eventually induced thrombus formation in ApoE KO mice

(A) Representative picture of the spontaneous thrombus in the left ventricle of Favine/ApoE DKO mice fed the Western diet for 4 months.

(B) Representative HE stain of heart sections containing thrombus.

(C) Representative HE stains of sham or ligated arteries from ApoE KO mice and ligated arteries from Favine/ApoE DKO mice fed normal chow. Scale bars are 200 μm. RA, right atrium; LA, left atrium; LV, left ventricle.

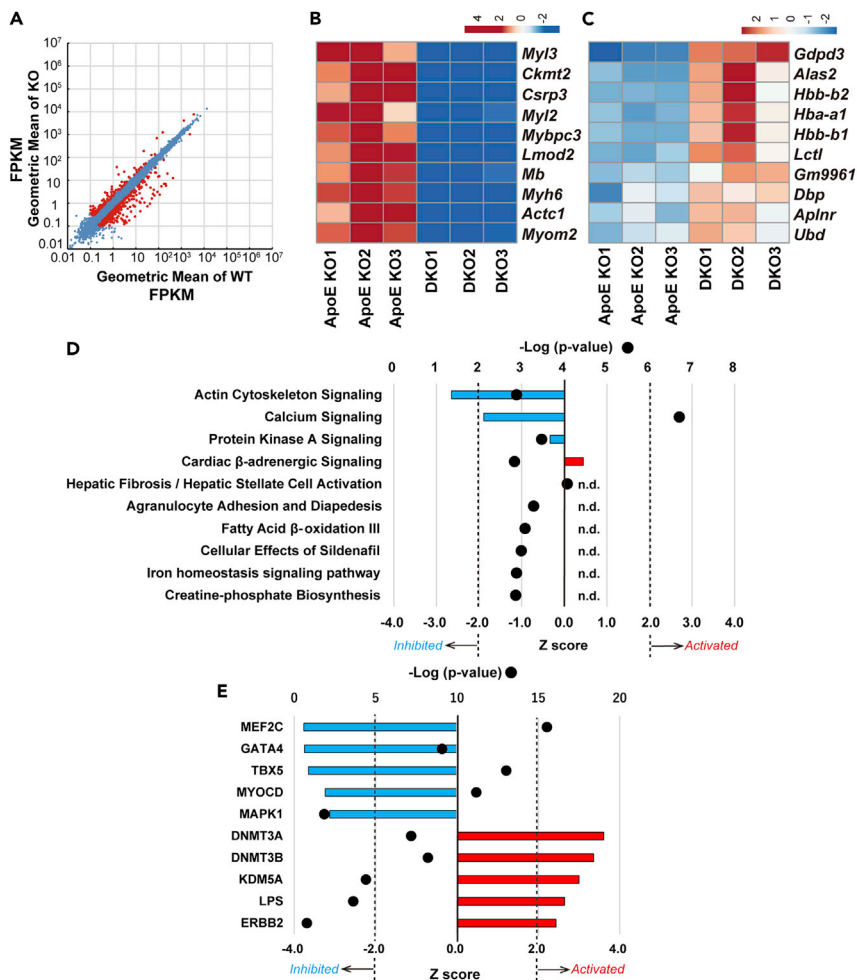


Figure 3. RNA-Seq analysis of aortae from ApoE KO mice and Favine/ApoE DKO mice fed normal chow for 1 year (A) Scatter plots of expressed genes in the aorta of ApoE KO mice and Favine/ApoE DKO mice in fragments per kilobase of transcript per million mapped reads (FPKM) are shown. Differentially expressed genes (DEGs) (red = significant, blue = nonsignificant).

(B and C) The most downregulated DEGs in DKO mice compared with ApoE KO mice (B) and the most upregulated DEGs (C). Differences between the two groups were examined for statistical significance using Student's *t*-test. The color scale shows log-transformed expression value, representing the mRNA expression level of each gene in blue (low)-red (high). (D) The significantly altered canonical pathways between ApoE KO mice and DKO mice (*n* = 3 each) are suggested by Ingenuity pathway analysis (IPA). The significance score (negative log of the *p*-value calculated by Fisher exact test) for each pathway is indicated by black dots. Blue columns refer to predicted inhibited pathways, whereas red color bars denote activated pathways based on z-score values. n.d. indicates z-scores are unavailable. The entries that have a $-\log(p\text{-value}) > 1.5$ are displayed. A dotted line indicates the z-score threshold.

(E) Predicted upstream regulators supplied by IPA in the aortae of DKO mice. The *p*-values (black dots) reflect the significance of enrichment. Blue columns refer to predicted inhibition, whereas red color bars denote activated, based on z-score values. A dotted line indicates the z-score threshold. See also [Figures S4–S7](#) and [Tables S1–S3](#).

that indicate that the probability of the association between a set of genes in our dataset and a biological function is significant. The two most robust functional differences were calcium signaling and actin cytoskeleton signaling, both of which were inhibited.

The upstream regulator analysis supplied by IPA can predict potential upstream regulators, including transcription factors, any gene, and a small molecule that have been observed experimentally to affect gene expression ([Kramer et al., 2014](#)). As shown in [Figure 3E](#), IPA predicted several decreased upstream regulators, including myocyte-specific enhancer factor 2c (MEF2C), T-box transcription factor 5 (TBX5),

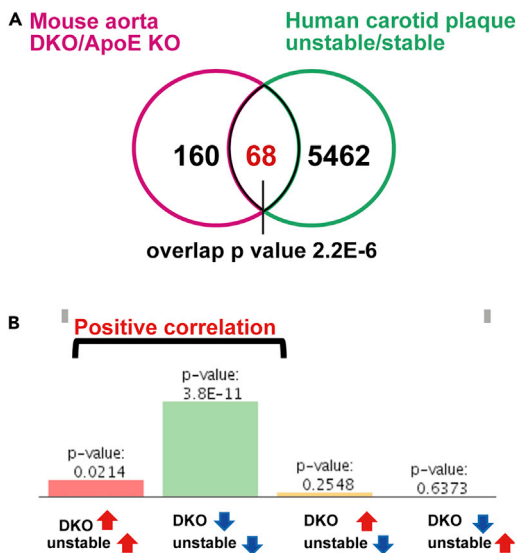


Figure 4. The correlation of the gene expression changes in aortae from Favine/ApoE DKO mice with those in human carotid arteries with unstable atherosclerosis

The DEGs in aortae from ApoE KO mice and Favine/ApoE DKO mice were compared with those in human carotid arteries with stable and unstable atherosclerosis (GEO DataSets: GSE120521) using BioSpace analysis. (A) The Venn diagram shows the number of common and unique genes in both sets. (B) The significance of the overlap between gene subsets. The scale of the bar is measured in $-\log(p\text{-value})$, which implies the higher the bar, the stronger the significance of the gene overlap.

myocardin (MYOCD), and GATA-binding protein 4 (GATA4) (Figure 3E, blue). These transcription factors are known to play critical roles in cardiovascular regulation (Dong et al., 2017; Potthoff and Olson, 2007; Sacilotto et al., 2016; Xu et al., 2015). Especially, gene expression levels of many MEF2C-targeting molecules were decreased in our RNA-Seq (Table S3). IPA also predicted several increased potential upstream regulators, including DNA methyltransferase 3 beta (DNMT3B), DNA methyltransferase 3 alpha (DNMT3A), lysine demethylase 5A (KDM5A), lipopolysaccharide and Erb-B2 receptor tyrosine kinase 2 (ERBB2) (Figure 3E, red).

Next, we performed a correlation analysis using the BioSpace Correlation Engine. Genes differentially expressed between DKO mice and ApoE KO mice were compared with those in unstable and stable regions dissected from fresh human carotid plaques obtained at carotid endarterectomy (GEO DataSets: GSE120521). Unstable regions in the human carotid artery contain vulnerable plaques with intraplaque hemorrhage. Correlation analysis indicated that gene expression changes in the aorta of DKO mice were correlated positively with those with unstable plaques in the human carotid artery ($p = 2.2 \text{ E-}6$) (Figure 4). As shown in Figure S5, there was considerable similarity between major canonical pathways in DKO mice and unstable plaques in the human carotid artery. Actin cytoskeleton signaling, integrin signaling, the GP6 signaling pathway, cardiac hypertrophy signaling, and calcium signaling were inhibited in both datasets.

Favine mRNA was decreased in human carotid atherosclerotic plaques

Actually, *FAVINE* expression was downregulated in atheroma plaques than in adjacent intact regions in the human carotid artery (Figure 5A). *FAVINE* mRNA expressions were also decreased during the progression of atherosclerosis (Figure 5B). Furthermore, *FAVINE* mRNA in human carotid unstable atherosclerotic plaque was decreased than those in stable plaque (Figure 5C).

Favine deficiency in endothelial cells attenuated MEF2C and KLF2 mRNA expression and increases PAI-1 expression

RNA-Seq suggested MEF2C as a potential upstream regulator of the atherosclerotic changes in the Favine-deficient aorta (Figure 3E and Table S3). MEF2C protects against the development of atherosclerosis by inhibiting TLR/NF- κ B activation, smooth muscle cell (SMC) migration, (Lu et al., 2017), and proliferation (Zhao et al., 2002). Kruppel-like Factor 2 (KLF2) is a downstream factor of MEF2C and inhibits atherosclerosis and thrombosis (Fan et al., 2017; Lu et al., 2017; Novodvorsky and Chico, 2014; Xu et al., 2015). Although neither murine *Mef2c* nor *Klf2* mRNA expression levels themselves in the whole aorta in our RNA-Seq data were altered between genotypes (Figure S6), expression levels of *FAVINE* and *MEF2C* mRNA were positively correlated in human carotid arteries (Figure 5D), suggesting the association of Favine with MEF2C-regulating pathway. To

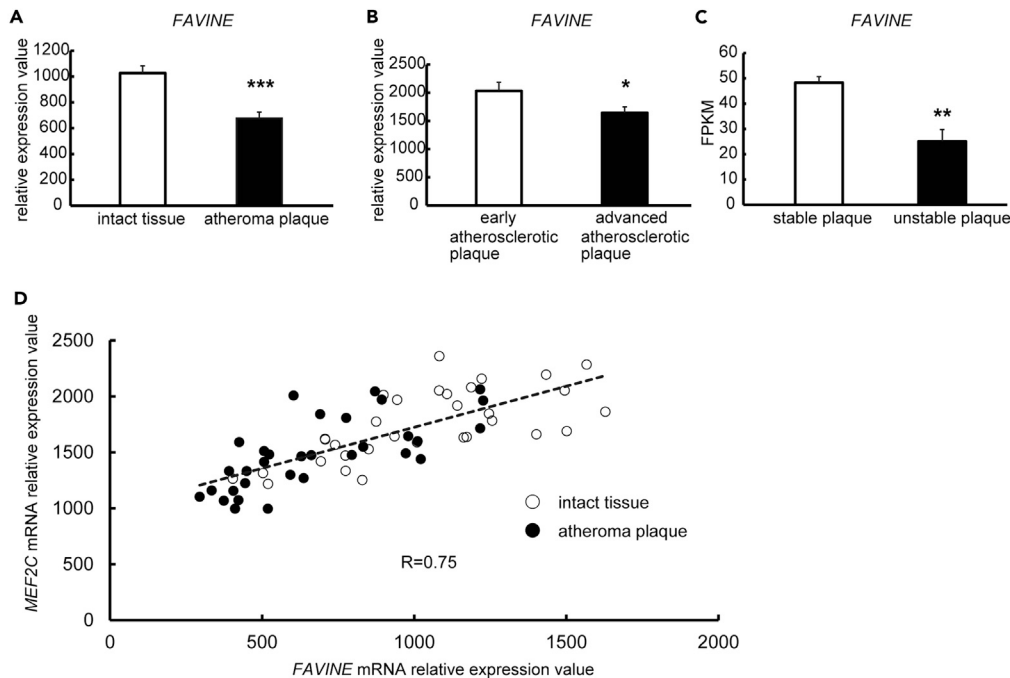


Figure 5. FAVINE mRNA expression in human carotid atherosclerotic plaque

(A) FAVINE mRNA expressions in human carotid atherosclerotic plaque and those in distant intact tissues collected from pieces of carotid endarterectomy in 32 patients. The data were obtained from GEO DataSets: GSE43292.

(B) FAVINE mRNA expression levels in human carotid advanced atherosclerotic segments and those in early atherosclerotic segments ($n = 16$ each). The data were obtained from GEO DataSets: GSE28829.

(C) FAVINE mRNA expression levels in human carotid unstable atherosclerotic plaque and those in stable plaque ($n = 4$ each). The data were obtained from GEO DataSets: GSE120521. Data are mean \pm SEM. * $p < 0.05$; ** $p < 0.01$; *** $p < 0.001$ by Student's t -test (A-C).

(D) Expression levels and FAVINE and MEF2C mRNA in human carotid arteries. Open circles indicate intact tissues. Closed circles indicate atheroma plaques. The data were obtained from GEO DataSets: GSE43292. See also Figure S1.

further elucidate the potential mechanism of the antiatherosclerotic effect of Favine, we investigated the possible Favine-MEF2C pathway. As shown in Table 3, Favine deficiency in the murine aorta downregulated the MEF2C/KLF2 regulatory pathway and partially upregulated TGF- β pathway-related genes such as *Irf7*, *Smad9*, and *Pai-1* (also known as *Serpine1*), which promote atherosclerosis, and increased the expression of a calcification-related gene, *Hmgb2*. Augmentation of the mRNA expression levels of prothrombotic factors, such as *Pai-1* and *F2rl3* (also known as *Protease-activated receptor 4 (Par-4)*) and decrease of antithrombotic factors, such as Thrombomodulin (*Thbd*) and *t-PA* was also observed in Favine/ApoE DKO mice. Above these gene expression changes might result in spontaneous thrombus formation in DKO mice. To confirm these RNA-Seq data, we carried out real-time RT-PCR using primers indicated (Table 4). An increase of *Pai-1* and a decrease of *t-PA* and *Thbd* were validated (Figure 6). Changes in *Irf7*, *Smad9*, *Hmgb2*, and *F2rl3* mRNA levels were not altered with significant differences between genotypes (Figure S7).

Based on these findings, we analyzed the effects of siRNA-mediated Favine knockdown in human umbilical vein endothelial cells (HUVECs). As shown in Figure 7, the knockdown of FAVINE resulted in a significant reduction in the mRNA levels of MEF2C and KLF2, which was associated with an increase in PAI-1 mRNA and a decrease in THBD mRNA. The downregulation of the MEF2C-KLF2-PAI-1/thrombomodulin pathway via Favine knockdown in HUVECs may at least partially explain the mechanisms of the development of atherosclerosis and thrombosis associated with Favine deficiency in mice.

DISCUSSION

Favine deficiency in apoE KO mice accelerated atherosclerosis accompanied by cholesterol crystal accumulation, arterial calcification, and spontaneous thrombus formation, all resembling the unstable

Table 3. Effects of favine deficiency on gene expression in the aorta

genes	Fold Change	p-value
Vascular tone		
<i>Edn1</i> *	1.3	n.s.
<i>Nos3</i> *	1.1	n.s.
Atherosclerosis		
<i>Irf7</i>	1.6	0.045
<i>Smad9</i>	1.5	0.036
<i>Pai-1</i> *	1.8	0.005
Calcification		
<i>Bglap</i> *	2.9	n.s.
<i>Hmgb2</i>	1.5	0.015
<i>Sost</i>	-1.1	n.s.
<i>Sox9</i> *	-1.1	n.s.
Thrombosis		
Pro-Thrombotic		
<i>Serpine1</i> *	1.8	0.005
<i>F2rl3</i> *	2.3	0.036
Anti-thrombotic		
<i>Thbd</i> *	-1.3	0.016
tPA*	-1.3	0.041

ApoE mice and DKO mice were fed normal chow for 1 year ($n = 3$ for ApoE KO and $n = 3$ for DKO mice). Data are fold change of FPKM (DKO/ApoE KO) in RNA-Seq. Differences between the two groups were examined for statistical significance using Student's t-test. *Genes marked with asterisk belong to MEF2C and/or KLF2-regulated genes. n.s., not significant. See also [Figures S7](#) and [S8](#).

plaques in human atherosclerotic arteries. Exaggerated atherosclerosis in DKO mice was independent of the severity of hyperglycemia, hyperinsulinemia, and dyslipidemia. The gene expression changes in the aorta of DKO mice resembled those with unstable plaques in the human carotid artery. Canonical pathway analysis revealed that calcium signaling and actin cytoskeleton signaling were downregulated in the aortae of DKO mice. The upstream regulator analysis suggested that Favine regulated the MEF2C-KLF2-PAI-1/Thrombomodulin pathway, thereby functioning as an antiatherosclerotic agent. The loss of *FAVINE* in HUVECs also suggested that Favine regulated this pathway ([Figure 7](#)). Although neither *Mef2c* nor *Klf2* mRNA expression levels themselves in the whole aorta in the RNA-seq were altered between genotypes ([Figure S6](#)), expression levels and *FAVINE* and *MEF2C* mRNA were positively correlated in atheroma plaque in human carotid arteries ([Figure 5D](#)). Furthermore, the knockdown of Favine in HUVEC resulted in significant attenuation of both *MEF2C* and *KLF2* genes themselves ([Figure 7](#)). Because endothelial cells are the small parts of cells in the total aorta, it might be difficult to affect gene expression levels in the whole aorta RNA-seq if *Mef2c* and *Klf2* were decreased only in the murine endothelial cells.

Nevertheless, the downstream gene expressions of the MEF2C/KLF2 pathway such as PAI-1 and Thrombomodulin were altered similarly between the total aorta and cultured endothelial cells, suggesting that the decreased MEF2C-KLF2 pathway was associated with Favine deficiency.

Vascular calcification is a marker of increased cardiovascular risk in aging and several diseases, including diabetes, atherosclerosis, and chronic kidney disease. Aortic calcification in wild-type mice is rare, and aortic calcification of ApoE KO mice occurs only in a specific lesion ([Nitschke et al., 2011](#); [Rattazzi et al., 2005](#)). Calcium signaling has been reported to control atherosclerosis susceptibility ([Mak et al., 2010](#); [Yuan et al., 2009](#)). Atherosclerosis itself differentially alters calcium signaling in the plaque-prone aortic arch to a greater extent than in the plaque-resistant thoracic aorta ([Prendergast et al., 2014](#)). However, the functional consequence of the downregulation of calcium signaling in atherosclerosis has not been

Table 4. Sequences of PCR primers used for real-time RT-PCR

	Forward	Reverse
m VCAM-1	GCTATGAGGATGGAAGACTCTGG	ACTTGTGCAGCCACCTGAGATC
m MCP-1	CCACTCACCTGCTGCTACTCAT	TGGTGATCCTCTTGCTAGCTCTCC
m TNF- α	TGTGCTCAGAGCTTTCAACAAC	GCCCATTGAGTCCTTGATG
m CD68	TGTCTGATCTTGCTAGGACCG	GAGAGTAACGGCCTTTTTGTGA
m PAI-1	TCAGCCCTTGCTTGCCCTCAT	GCATAGCCAGCACCGAGGA
m 36B4	GCTCCAAGCAGATGCAGCA	CCGGATGTGAGGCAGCAG
m ET1	GCACCGGAGCTGAGAATGG	GTGGCAGAAGTAGACACACTC
m Nos3	CCTTCCGCTACCAGCCAGA	CAGAGATCTTCACTGCATTGGCTA
m Irf7	GAGACTGGCTATTGGGGGAG	GACCGAAATGCTTCCAGGG
m Smad9	CGGGTCAGCCTAGCAAGTG	GAGCCGAACGGGAACCTCAC
m Bglap	ATTTAGGACCTGTGCTGCC	GGAGCTGCTGTGACATCCAT
m Hmgb2	CGGGGCAAAATGTCCTCGTA	ATGGTCTTCCATCTCTCGGAG
m Sost	AGCCTTCAGGAATGATGCCAC	CTTTGGCGTCATAGGGATGGT
m Sox9	AGTACCCGCATCTGCACAAC	ACGAAGGGTCTCTTCTCGCT
m F2rl3	CCGCTGCTGTATCCTTTGGT	TCCTTGAGTTCTACTGTGGGAC
m Thbd	CTCTCCGCACTAGCCAAGC	GGAGCGCACTGCATCAAATG
m tPA	TGACCAGGGAATACATGGGAG	CTGAGTGGCATTGTACCAGGC
h Favine	CCCAGACACTCAAGAGAACAGAAGG	TGGTCTCCTCCTCAAACAAGG
h MEF2C	GCCCTGAGTCTGAGGACAAG	AGTGAGCTGACAGGGTTGCT
h KLF-2	TTCGGTCTCTTCGACGACG	TGCGAACTCTTGGTGTAGGTC
h PAI-1	GGCTGACTTCACGAGTCTTTCAG	CGTTCACCTCGATCTTCACTTTC
h THBD	ACCTTCTCAATGCCAGTCAG	CGTCGCCGTTCACTAGCAA
h CYPA	ATGGTCAACCCACCGTGT	CTGCTGTCTTTGGGACCTTGTC

demonstrated. In the present study, Favine/ApoE DKO mice developed numerous calcification lesions, particularly in the aortic root. Inhibited calcium signaling was top predicted by the pathway analysis, suggesting that altered calcium signaling may predispose to vascular calcification in Favine/DKO mice. Upstream regulator analysis in RNA-Seq and *in vitro* endothelial Favine knockdown experiments suggested the possible signaling of Favine in the regulation of the MEF2C-KLF2-PAI-1/thrombomodulin pathway under atherogenic conditions (Figure 8).

Thrombus often develops at the site of disrupted atherosclerotic plaques in humans. However, to our knowledge, thrombi do not form spontaneously in mice. Even in ApoE KO mice and PAI-1 KO mice, stimuli such as laser induction or ferric chloride treatment are required to induce thrombus (Cherpokova and Nieswandt, 2017; Westrick et al., 2007). In our experiments, left ventricular thrombi were spontaneously found in Favine/ApoE DKO mice without any stimulation. Favine/ApoE DKO mice also displayed thrombi at the ligated carotid arteries. KLF2 has antithrombotic roles by regulating endothelial thrombotic factors such as Thrombomodulin, t-PA, PAI-1, and PAR4 (Sangwung et al., 2017) and may contribute to thrombus formation in Favine/ApoE DKO mice.

PAI-1 deficiency in ApoE KO mice is known to accelerate atherosclerosis in mice (Xiao et al., 1997). In ApoE KO mice, PAI-1 expression in endothelial cells in advanced atherosclerotic lesions is upregulated, and deletion of the *Pai-1* gene reduces neointimal growth after injury despite the persistence of excessive hypercholesterolemia (Schafer et al., 2003). Endothelial KLF2 knockdown induces PAI-1 expression (Lin et al., 2005). KLF2 overexpression in HUVECs suppresses PAI-1 expression (Boon et al., 2007). Considering these reports, the increased PAI-1 in Favine deficiency could be a consequence of decreased KLF2 expression. In agreement with our supposition, Favine mRNA was decreased in the aortic roots in young Klotho-KO mice (GEO DataSets: GSE52794, Figure S8). Klotho KO mice are well known to possess a severe senescent phenotype, including atherosclerotic and calcified changes in vessels (Olejnik et al., 2018). PAI-1 is elevated in Klotho KO mice, and PAI-1 deficiency counteracts the

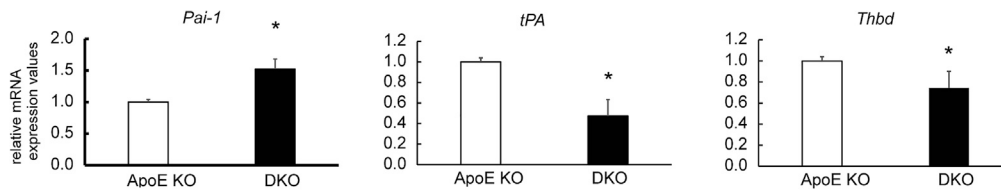


Figure 6. The changes of gene expression in the aorta of ApoE KO and DKO mice

ApoE mice and DKO mice were fed normal chow for 1 year ($n = 6$ for ApoE KO and $n = 4$ for DKO mice). The mRNA expression levels were normalized against the *36B4* level. Data are mean \pm SEM. Differences between the two groups were examined for statistical significance using Student's *t*-test. * $p < 0.05$ by Student's *t*-test.

development of senescent phenotypes (Eren et al., 2014). PAI-1 might be a key factor in the enhancement of atherosclerosis and calcification in Favine-deficient aortae.

A single nucleotide polymorphism around the *FAVINE* gene (rs525455) is strongly associated with ADP-induced platelet aggregation in two human cohort studies (Framingham Heart Study and Genetic Study of Atherosclerosis Risk) (Johnson et al., 2010). *FAVINE* SNP is among the top 5 SNPs related to platelet aggregation in human subjects (Johnson et al., 2010). We found spontaneous left ventricular thrombus formation and thrombi at the ligated carotid arteries in Favine/ApoE DKO mice. The lack of a sufficient amount of Favine may predispose to platelet aggregation and thrombus formation in both mice and humans.

In our previous study, we showed that Favine is a secreted factor (Kobayashi et al., 2010). Now, we have developed new monoclonal IgG antibodies and are developing a sandwich enzyme-linked immunosorbent assay (EIA) for measuring murine Favine in biological fluids (Figure S9). Our preliminary measurement of Favine in plasma gave positive values, ranging from 40 to 80 pg/mL in WT mice and no detection in KO mice (Table S4). This may further support the hypothesis that Favine is a secreted factor circulating in the blood.

Altogether, our study revealed that Favine was required to maintain vascular homeostasis, at least partly through the MEF2C-KLF2 pathway. The unique resemblance of human unstable plaques in terms of the gene expression signatures and the association of calcification and thrombus formation highlights Favine among the known humoral factors in the development of atherosclerosis. Favine and its downstream pathways may have therapeutic potential for atherosclerosis.

Limitations of the study

As far as we analyzed the whole aorta RNA expressions of DKO mice, we could not find any differences in gene expression of inflammatory genes compared with ApoE KO mice. However, the contribution of

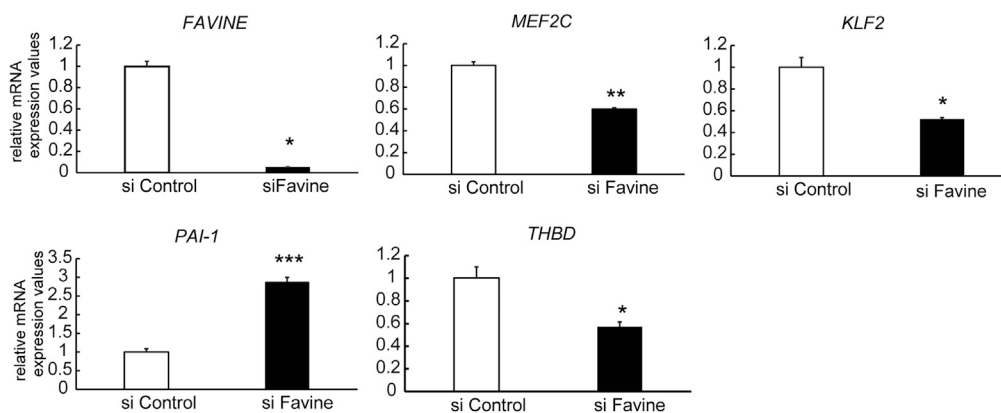


Figure 7. The changes of MEF2C-KLF2 pathway genes in cultured endothelial cells by Favine knockdown

HUVEC gene expressions were evaluated 24 h after transfections of control siRNA and Favine siRNA. The mRNA expression levels were normalized against the *CYP4* level. Data are mean \pm SEM. * $p < 0.05$; ** $p < 0.01$; *** $p < 0.001$ by the Student's *t*-test.

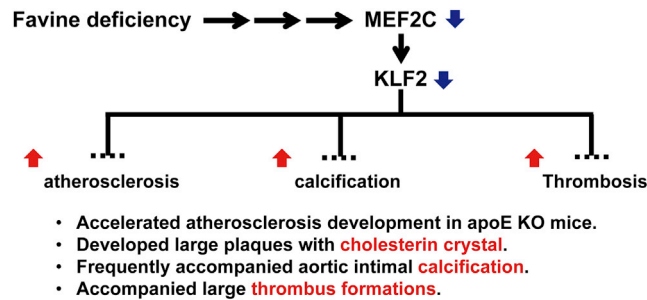


Figure 8. Proposed Favine-regulating pathway

inflammation by immune cell infiltration has not been fully analyzed in this study. Single-cell RNA analysis in aortae of DKO mice may provide more precise information in the future.

Although we demonstrated the presence of Favine in the plasma of WT mice, the existence in plasma alone cannot prove that Favine functions as a soluble factor. Whether the supplementation of Favine in circulation can rescue severe atherosclerosis found in DKO mice will answer this question in the future.

The precise mechanisms through which Favine-deficiency accelerated atherosclerosis progression and decreased MEF2C-KLF2 transcriptional pathway have not been answered yet. Time-course analysis of atherosclerosis progression in DKO mice and supplementation of Favine in DKO mice may reveal the issues partly.

Whether the spontaneous thrombus formation in DKO mice relies on the activation of endothelium, platelets, or both has not been addressed yet. A study on platelet activation may be required for answering this question.

We found that the human *FAVINE* mRNA expressions were lower in atheroma plaque than in adjacent intact aortic tissue and decreased with the progression of atherosclerosis. The regulation of *Favine* mRNA expression in specific cell types such as endothelial cell and smooth muscle cells must be studied in the future.

Favine is expressed both in the aorta and fat tissues. Metabolic disorders such as obesity and diabetes are also well-known risk factors for atherosclerosis. The interorgan crosstalk between fat tissues and aorta modulated by Favine should be revealed in a future study.

STAR★METHODS

Detailed methods are provided in the online version of this paper and include the following:

- KEY RESOURCES TABLE
- RESOURCE AVAILABILITY
 - Lead contact
 - Materials availability
 - Data and code availability
- EXPERIMENTAL MODEL AND SUBJECT DETAILS
 - Animals
 - Cell cultures
- METHOD DETAILS
 - Oil Red O Stain of the aorta
 - Hematoxylin and eosin staining
 - Measurement of cholesterol clefts
 - von Kossa calcium stain
 - Real-time RT-PCR analysis
 - RNA-seq analysis
 - Carotid artery ligation

- Analysis of Human Favine/CCDC3 expression
- Measurement of murine Favine concentration
- **QUANTIFICATION AND STATISTICAL ANALYSIS**
- Statistics

SUPPLEMENTAL INFORMATION

Supplemental information can be found online at <https://doi.org/10.1016/j.isci.2022.105252>.

ACKNOWLEDGMENTS

We thank Takako Sawamura, Misako Kobayashi, and Haruyo Sakamoto for their technical assistance. We thank Takuya Yoshida for the helpful discussions. We also thank the staff of the Center of Medical Research and Education and Institute of Experimental Animal Sciences, Graduate School of Medicine Osaka University for excellent technical support and assistance. This work was supported by Grants-in-aid for Young Scientists 25860767 and 16K19554, Grants-in-Aid for Scientific Research 15H04853, 18H02863, 19K09001, and 22K08624 from the Japan Society for the Promotion of Science, and a grant from the Japan Foundation for Applied Enzymology and MSD Life Science Foundation.

AUTHOR CONTRIBUTIONS

Conceptualization, S.Kobayashi., S.Kita., A.F., Y.N., E.M., and I.S.; investigation, S.Kobayashi., S.Kita., H.K., and D.O.; writing – original draft, S.Kobayashi. and S.Kita.; writing – review and editing, E.M. and I.S.; funding acquisition, S.Kobayashi. and I.S.; resources, S.Kobayashi., H.K., O.D., and E.M.; data curation, O.D.; supervision, I.S.

S.Kobayashi. and S.Kita. designed the research protocol, performed the biochemical, cellular, and *in vivo* experiments, analyzed the data, and co-wrote the manuscript. D.O. assisted with the pathway analysis and performed data curations. H.K. analyzed the thrombus. Y.F. assisted in experiments of murine carotid artery ligation. K.M. performed antibody screening and established and validated the new Favine ELISA. C.Y. assisted in experiments of the Favine ELISA measurements. E.M. performed histological analysis. The manuscript was written by S.Kobayashi. and S.Kita., reviewed, and edited by E.M., A.F., and I.S. All studies were supervised by I.S.

DECLARATION OF INTERESTS

A.F. and S.Kita. belong to the endowed department by Takeda Pharmaceutical Company, Rohto Pharmaceutical Co., Ltd., Sanwa Kagaku Kenkyusho Co., Ltd., FUJI OIL HOLDINGS INC., and Kobayashi Pharmaceutical Co., Ltd.

The funders had no role in the study design, data collection and analysis, decision to publish, or preparation of the manuscript.

All other authors declare no competing interests.

Received: November 5, 2021

Revised: August 1, 2022

Accepted: September 28, 2022

Published: November 18, 2022

REFERENCES

- Angulo, J., Nguyen-Khoa, T., Massy, Z.A., Drüeke, T., and Serra, J. (2011). Morphological quantification of aortic calcification from low magnification images. *Image Anal. Stereol.* **22**, 81. <https://doi.org/10.5566/ias.v22.p81-89>.
- Ayari, H., and Bricca, G. (2013). Identification of two genes potentially associated in iron-heme homeostasis in human carotid plaque using microarray analysis. *J. Biosci.* **38**, 311–315. <https://doi.org/10.1007/s12038-013-9310-2>.
- Boon, R.A., Fledderus, J.O., Volger, O.L., van Wanrooij, E.J.A., Pardali, E., Weesie, F., Kuiper, J., Pannekoek, H., ten Dijke, P., and Horrevoets, A.J.G. (2007). KLF2 suppresses TGF-beta signaling in endothelium through induction of Smad7 and inhibition of AP-1. *Arterioscler. Thromb. Vasc. Biol.* **27**, 532–539. <https://doi.org/10.1161/01.ATV.0000256466.65450.ce>.
- Cherpokova, D., and Nieswandt, B. (2017). Mouse models of thrombosis. In *Platelets in Thrombotic and Non-Thrombotic Disorders* (Springer International Publishing), pp. 681–698. https://doi.org/10.1007/978-3-319-47462-5_46.

- Doherty, T.M., Asotra, K., Fitzpatrick, L.A., Qiao, J.-H., Wilkin, D.J., Detrano, R.C., Dunstan, C.R., Shah, P.K., and Rajavashisth, T.B. (2003). Calcification in atherosclerosis: bone biology and chronic inflammation at the arterial crossroads. *Proc. Natl. Acad. Sci. USA* 100, 11201–11206. <https://doi.org/10.1073/pnas.1932554100>.
- Dong, C., Yang, X.Z., Zhang, C.Y., Liu, Y.Y., Zhou, R.B., Cheng, Q.D., Yan, E.K., and Yin, D.C. (2017). Myocyte enhancer factor 2C and its directly-interacting proteins: a review. *Prog. Biophys. Mol. Biol.* 126, 22–30. <https://doi.org/10.1016/j.biombio.2017.02.002>.
- Döring, Y., Manthey, H.D., Drechsler, M., Lievens, D., Megens, R.T.A., Soehnlein, O., Busch, M., Manca, M., Koenen, R.R., Pelisek, J., et al. (2012). Auto-antigenic protein-DNA complexes stimulate plasmacytoid dendritic cells to promote atherosclerosis. *Circulation* 125, 1673–1683. <https://doi.org/10.1161/circulationaha.111.046755>.
- Eckel, R.H., Bornfeldt, K.E., and Goldberg, I.J. (2021). Cardiovascular disease in diabetes, beyond glucose. *Cell Metab.* 33, 1519–1545. <https://doi.org/10.1016/j.cmet.2021.07.001>.
- Edgar, R., Domrachev, M., and Lash, A.E. (2002). Gene Expression Omnibus: NCBI gene expression and hybridization array data repository. *Nucleic Acids Res.* 30, 207–210. <https://doi.org/10.1093/nar/30.1.207>.
- Eren, M., Boe, A.E., Murphy, S.B., Place, A.T., Nagpal, V., Morales-Nebreda, L., Ulrich, D., Quaggin, S.E., Budinger, G.R.S., Mutlu, G.M., et al. (2014). PAI-1-regulated extracellular proteolysis governs senescence and survival in Klotho mice. *Proc. Natl. Acad. Sci. USA* 111, 7090–7095. <https://doi.org/10.1073/pnas.1321942111>.
- Fan, Y., Lu, H., Liang, W., Hu, W., Zhang, J., and Chen, Y.E. (2017). Krüppel-like factors and vascular wall homeostasis. *J. Mol. Cell Biol.* 9, 352–363. <https://doi.org/10.1093/jmcb/mjx037>.
- Johnson, A.D., Yanek, L.R., Chen, M.H., Faraday, N., Larson, M.G., Tofler, G., Lin, S.J., Kraja, A.T., Province, M.A., Yang, Q., et al. (2010). Genome-wide meta-analysis identifies seven loci associated with platelet aggregation in response to agonists. *Nat. Genet.* 42, 608–613. <https://doi.org/10.1038/ng.604>.
- Kobayashi, S., Fukuhara, A., Otsuki, M., Suganami, T., Ogawa, Y., Morii, E., and Shimomura, I. (2015). Fat/vessel-derived secretory protein (Favine)/CCDC3 is involved in lipid accumulation. *J. Biol. Chem.* 290, 7443–7451. <https://doi.org/10.1074/jbc.M114.592493>.
- Kobayashi, S., Fukuhara, A., Taguchi, T., Matsuda, M., Tochino, Y., Otsuki, M., and Shimomura, I. (2010). Identification of a new secretory factor, CCDC3/Favine, in adipocytes and endothelial cells. *Biochem. Biophys. Res. Commun.* 392, 29–35. <https://doi.org/10.1016/j.bbrc.2009.12.142>.
- Krämer, A., Green, J., Pollard, J., Jr., and Tugendreich, S. (2014). Causal analysis approaches in ingenuity pathway analysis. *Bioinformatics* 30, 523–530. <https://doi.org/10.1093/bioinformatics/btt703>.
- Langmead, B., and Salzberg, S.L. (2012). Fast gapped-read alignment with Bowtie 2. *Nat. Methods* 9, 357–359. <https://doi.org/10.1038/nmeth.1923>.
- Li, H., Handsaker, B., Wysoker, A., Fennell, T., Ruan, J., Homer, N., Marth, G., Abecasis, G., Durbin, R., and Subgroup, G.P.D.P. (2009). The Sequence Alignment/Map format and SAMtools. *Bioinformatics* 25, 2078–2079. <https://doi.org/10.1093/bioinformatics/btp352>.
- Lin, Z., Kumar, A., Senbanerjee, S., Staniszewski, K., Parmar, K., Vaughan, D.E., Gimbrone, M.A., Balasubramanian, V., García-Cardeña, G., and Jain, M.K. (2005). Kruppel-like factor 2 (KLF2) regulates endothelial thrombotic function. *Circ. Res.* 96, e48–e57. <https://doi.org/10.1161/01.res.0000159707.05637.a1>.
- Lu, Y.W., Lowery, A.M., Sun, L.Y., Singer, H.A., Dai, G., Adam, A.P., Vincent, P.A., and Schwarz, J.J. (2017). Endothelial myocyte enhancer factor 2c inhibits migration of smooth muscle cells through fenestrations in the internal elastic lamina. *Arterioscler. Thromb. Vasc. Biol.* 37, 1380–1390. <https://doi.org/10.1161/ATVBAHA.117.309180>.
- Mahmoud, A.D., Ballantyne, M.D., Miscianinov, V., Pinel, K., Hung, J., Scanlon, J.P., Iyinkkel, J., Kaczynski, J., Tavares, A.S., Bradshaw, A.C., et al. (2019). The human-specific and smooth muscle cell-enriched lncRNA SMILR promotes proliferation by regulating mitotic CENPF mRNA and drives cell-cycle progression which can be targeted to limit vascular remodeling. *Circ. Res.* 125, 535–551. <https://doi.org/10.1161/circresaha.119.314876>.
- Mak, S., Sun, H., Acevedo, F., Shimmin, L.C., Zhao, L., Teng, B.B., and Hixson, J.E. (2010). Differential expression of genes in the calcium-signaling pathway underlies lesion development in the LDb mouse model of atherosclerosis. *Atherosclerosis* 213, 40–51. <https://doi.org/10.1016/j.atherosclerosis.2010.06.038>.
- Mukai, Y., Rikitake, Y., Shiojima, I., Wolfrum, S., Satoh, M., Takeshita, K., Hiroi, Y., Salomone, S., Kim, H.H., Benjamin, L.E., et al. (2006). Decreased vascular lesion formation in mice with inducible endothelial-specific expression of protein kinase Akt. *J. Clin. Invest.* 116, 334–343. <https://doi.org/10.1172/jci26223>.
- Nicolli, R., and Heinein, M.Y. (2014). The predictive value of arterial and valvular calcification for mortality and cardiovascular events. *Int. J. Cardiol. Heart Vessel.* 3, 1–5. <https://doi.org/10.1016/j.ijchv.2014.02.001>.
- Nitschke, Y., Weissen-Plenz, G., Terkeltaub, R., and Rutsch, F. (2011). Npp1 promotes atherosclerosis in ApoE knockout mice. *J. Cell Mol. Med.* 15, 2273–2283. <https://doi.org/10.1111/j.1582-4934.2011.01327.x>.
- Novodvorsky, P., and Chico, T.J.A. (2014). The role of the transcription factor KLF2 in vascular development and disease. In *Prog. Mol. Biol. Transl. Sci.* (Elsevier), pp. 155–188. <https://doi.org/10.1016/b978-0-12-386930-2.00007-0>.
- Olejnik, A., Franczak, A., Krzywonos-Zawadzka, A., Kałużna-Oleksy, M., and Bil-Lula, I. (2018). The biological role of Klotho protein in the development of cardiovascular diseases. *BioMed Res. Int.* 2018, 5171945. <https://doi.org/10.1155/2018/5171945>.
- Plump, A.S., Smith, J.D., Hayek, T., Aalto-Setälä, K., Walsh, A., Verstuyft, J.G., Rubin, E.M., and Breslow, J.L. (1992). Severe hypercholesterolemia and atherosclerosis in apolipoprotein E-deficient mice created by homologous recombination in ES cells. *Cell* 71, 343–353. [https://doi.org/10.1016/0092-8674\(92\)90362-g](https://doi.org/10.1016/0092-8674(92)90362-g).
- Potthoff, M.J., and Olson, E.N. (2007). MEF2: a central regulator of diverse developmental programs. *Development* 134, 4131–4140. <https://doi.org/10.1242/dev.008367>.
- Prendergast, C., Quayle, J., Burduga, T., and Wray, S. (2014). Atherosclerosis differentially affects calcium signalling in endothelial cells from aortic arch and thoracic aorta in Apolipoprotein E knockout mice. *Physiol. Rep.* 2, e12171. <https://doi.org/10.14814/phy2.12171>.
- Rattazzi, M., Bennett, B.J., Bea, F., Kirk, E.A., Ricks, J.L., Speer, M., Schwartz, S.M., Giachelli, C.M., and Rosenfeld, M.E. (2005). Calcification of advanced atherosclerotic lesions in the innominate arteries of ApoE-deficient mice. *Arterioscler. Thromb. Vasc. Biol.* 25, 1420–1425. <https://doi.org/10.1161/01.atv.0000166600.58468.1b>.
- Sacilotto, N., Chouliaras, K.M., Nikitenko, L.L., Lu, Y.W., Fritzsche, M., Wallace, M.D., Nornes, S., García-Moreno, F., Payne, S., Bridges, E., et al. (2016). MEF2 transcription factors are key regulators of sprouting angiogenesis. *Genes Dev.* 30, 2297–2309. <https://doi.org/10.1101/gad.290619.116>.
- Sangwung, P., Zhou, G., Nayak, L., Chan, E.R., Kumar, S., Kang, D.-W., Zhang, R., Liao, X., Lu, Y., Sugi, K., et al. (2017). KLF2 and KLF4 control endothelial identity and vascular integrity. *JCI Insight* 2, e91700. <https://doi.org/10.1172/jci.insight.91700>.
- Schafer, K., Muller, K., Hecke, A., Mounier, E., Goebel, J., Loskutoff, D.J., and Konstantinides, S. (2003). Enhanced thrombosis in atherosclerosis-prone mice is associated with increased arterial expression of plasminogen activator inhibitor-1. *Arterioscler. Thromb. Vasc. Biol.* 23, 2097–2103. <https://doi.org/10.1161/01.ATV.0000097766.36623>.
- Schneider, C.A., Rasband, W.S., and Eliceiri, K.W. (2012). NIH Image to ImageJ: 25 years of image analysis. *Nat. Methods* 9, 671–675. <https://doi.org/10.1038/nmeth.2089>.
- Trapnell, C., Pachter, L., and Salzberg, S.L. (2009). TopHat: discovering splice junctions with RNA-Seq. *Bioinformatics* 25, 1105–1111. <https://doi.org/10.1093/bioinformatics/btp120>.
- Trapnell, C., Roberts, A., Goff, L., Pertea, G., Kim, D., Kelley, D.R., Pimental, H., Salzberg, S.L., Rinn, J.L., and Pachter, L. (2012). Differential gene and transcript expression analysis of RNA-seq experiments with TopHat and Cufflinks. *Nat. Protoc.* 7, 562–578. <https://doi.org/10.1038/nprot.2012.016>.
- Trapnell, C., Williams, B.A., Pertea, G., Mortazavi, A., Kwan, G., Van Baren, M.J., Salzberg, S.L., Wold, B.J., and Pachter, L. (2010). Transcript assembly and quantification by RNA-Seq reveals unannotated transcripts and isoform switching

during cell differentiation. *Nat. Biotechnol.* 28, 511–515. <https://doi.org/10.1038/nbt.1621>.

Westrick, R.J., Winn, M.E., and Eitzman, D.T. (2007). Murine models of vascular thrombosis (Eitzman series). *Arterioscler. Thromb. Vasc. Biol.* 27, 2079–2093. <https://doi.org/10.1161/ATVBAHA.107.142810>.

Wolf, D., and Ley, K. (2019). Immunity and inflammation in atherosclerosis. *Circ. Res.* 124, 315–327. <https://doi.org/10.1161/circresaha.118.313591>.

Xiao, Q., Danton, M.J., Witte, D.P., Kowala, M.C., Valentine, M.T., Bugge, T.H., and Degen, J.L. (1997). Plasminogen deficiency accelerates vessel

wall disease in mice predisposed to atherosclerosis. *Proc. Natl. Acad. Sci. USA* 94, 10335–10340. <https://doi.org/10.1073/pnas.94.19.10335>.

Xu, Z., Yoshida, T., Wu, L., Maiti, D., Cebotaru, L., and Duh, E.J. (2015). Transcription factor MEF2C suppresses endothelial cell inflammation via regulation of NF-kappaB and KLF2. *J. Cell. Physiol.* 230, 1310–1320. <https://doi.org/10.1002/jcp.24870>.

Yahagi, K., Kolodgie, F.D., Lutter, C., Mori, H., Romero, M.E., Finn, A.V., and Virmani, R. (2017). Pathology of human coronary and carotid artery atherosclerosis and vascular calcification in diabetes mellitus. *Arterioscler. Thromb. Vasc.*

Biol. 37, 191–204. <https://doi.org/10.1161/atvbaha.116.306256>.

Yuan, Z., Miyoshi, T., Bao, Y., Sheehan, J.P., Matsumoto, A.H., and Shi, W. (2009). Microarray analysis of gene expression in mouse aorta reveals role of the calcium signaling pathway in control of atherosclerosis susceptibility. *Am. J. Physiol. Heart Circ. Physiol.* 296, H1336–H1343. <https://doi.org/10.1152/ajpheart.01095.2008>.

Zhao, M., Liu, Y., Bao, M., Kato, Y., Han, J., and Eaton, J.W. (2002). Vascular smooth muscle cell proliferation requires both p38 and BMK1 MAP kinases. *Arch. Biochem. Biophys.* 400, 199–207. [https://doi.org/10.1016/s0003-9861\(02\)00028-0](https://doi.org/10.1016/s0003-9861(02)00028-0).

STAR★METHODS

KEY RESOURCES TABLE

REAGENT or RESOURCE	SOURCE	IDENTIFIER
Chemicals, peptides, and recombinant proteins		
MCDB131 medium	Gibco	Cat #10372019
Fetal bovine serum	Equitech-Bio	Cat #SFBM30-500
Human fibroblast growth factor	Biovision	Cat #4037-50
Lipofectamine RNAiMax Transfection Reagent	Thermo Fisher Scientific	Cat #13778150
EBM-2 medium	Lonza	Cat #00190860
TRI Reagent	Sigma-Aldrich	Cat #T9424-200ML
FastStart Essential DNA Green Master	Roche	Cat #06924204001
PrimeScript Reverse Transcriptase	TAKARA	Cat #2680A
4% buffered formaldehyde	Nacalai	Cat #37152-64
Oil red O	Nacalai	Cat #25633-92
Critical commercial assays		
Calcium stain kit	Scy Tek Laboratories	Cat #CVK-1
TruSeq Stranded mRNA Sample Prep Kit	Illumina	Cat #20020594
CII-test kit	Wako Pure Chemical Industries	Cat #439-90901
triglyceride E-test	Wako Pure Chemical Industries	Cat #432-40201
T-CHO E-test	Wako Pure Chemical Industries	Cat #439-17501
insulin enzyme-linked immunoassay kit	Morinaga	Cat #M1104
calcium E-test	Wako Pure Chemical Industries	Cat #437-58201
L type Wako IP	Wako Pure Chemical Industries	Cat #462-45101
PAI-1 total antigen ELISA kit	Molecular Innovations	Cat #MPAIKT-TOT
Favine ELISA kit	This paper	N/A
Deposited data		
RNA-Seq data	This paper	GEO DataSets: GSE183376
Raw Data	This paper	https://data.mendeley.com/datasets/mn3hxx9dd/draft?a=5c6d9cba-49e8-4fda-a658-76c522aeb671
Experimental models: Cell lines		
Human: HUVEC	Kurabo	Cat# FC-0044
Experimental models: Organisms/strains		
Mouse: C57BL/6J-Favine $-/-$	Kobayashi et al. (2015)	N/A
Mouse: B6.129P2-Apoe ^{tm1Unc/J}	The Jackson Laboratory	RRID:IMSR_JAX:002052; https://www.jax.org/strain/002052
Mouse: C57BL/6J- Favine $-/-$ ApoE $-/-$	This paper	N/A
Mouse: C57BL/6J	CLEA	RRID:IMSR_JAX:000664; https://www.clea-japan.com/products/inbred/item_a0420
Oligonucleotides		
RNA targeting human Favine	Ambion	Cat#4427037
nontargeting control siRNA	Ambion	Cat#4390846
Primers for real-time RT-PCR, see Table 4	This paper	N/A

(Continued on next page)

Continued

REAGENT or RESOURCE	SOURCE	IDENTIFIER
<i>Software and algorithms</i>		
Image J	Schneider et al. (2012)	https://imagej.nih.gov/ij/
BioZero X-Analyzer software	Keyence	https://www.keyence.co.jp/products/microscope/fluorescence-microscope/bz-x700/models/bz-h3m/
JMP Pro 15	SAS Institute	https://support.sas.com/downloads/index.htm?fil=2
Illumina CASAVA version 1.8.2 software	Illumina, San Diego, CA, USA	N/A
TopHat version 2.0.13	Trapnell et al., 2009, 2012	https://ccb.jhu.edu/software/tophat/index.shtml
Bowtie2 version 2.2.3	Langmead and Salzberg (2012)	http://www.bowtie-bio.sourceforge.net/bowtie2/index.shtml
SAMtools version 0.1.19	Li et al., 2009	http://samtools.sourceforge.net/
Cuffnorm version 2.2.1	Trapnell et al. (2010)	http://cole-trapnell-lab.github.io/cufflinks/manual/
IPA	QIAGEN Redwood City, CA, USA	http://www.qiagen.com/ingenuity
Basespace Correlation Engine	Illumina, San Diego, CA, USA	https://support.illumina.com/sequencing/sequencing_software/basespace-correlation-engine.html
LightCycler 96 instrument	Roche	https://lifescience.roche.com/global_en/products/lightcycler-381711.html

RESOURCE AVAILABILITY

Lead contact

Further information and requests for resources and reagents should be directed to and will be fulfilled by the lead contact, Sachiko Kobayashi (skobayashi@endmet.med.osaka-u.ac.jp).

Materials availability

The materials underlying this article will be shared upon reasonable request to the the [lead contact](#), Sachiko Kobayashi.

Data and code availability

- The raw data obtained in RNA-Seq in this study was submitted under Gene Expression Omnibus (GEO) accession number GEO DataSets: GSE183376. Microscopy data reported in this paper will be shared by the [lead contact](#) upon request.
- This paper does not report original code.
- Any additional information required to reanalyze the data reported in this paper is available from the [lead contact](#) upon request.

EXPERIMENTAL MODEL AND SUBJECT DETAILS

Animals

We generated Favine/ApoE double KO mice. Favine-deficient mice were bred with ApoE-deficient mice to generate single (ApoE $-/-$, Favine $-/-$) and combined (ApoE $-/-$ /Favine $-/-$) deficiencies in ApoE and Favine. The mice had *ad libitum* access to water and chow (MF, Oriental Yeast, Suita, Japan). For the atherosclerosis-prone conditions, mice were fed a Western diet containing 34% sucrose, 20% butter, and 0.15% Cholesterol (Oriental Yeast, Suita, Japan). All experimental western diet feeding was started at 6 weeks old. All animals were housed in a temperature-controlled room under a 12-h light/12-h dark cycle. The animals were weighed at 10 a.m. in the fed state. We used male mice for the western diet study and female mice for 1-year study fed with normal chow. The mice were sacrificed at 1 p.m. Tissues from each mouse were dissected and washed with phosphate-buffered saline (PBS). Following immediate weighing, the tissues were snap-frozen in liquid nitrogen or fixed in 4% buffered formaldehyde. ApoE KO mice, Favine/ApoE DKO mice, C57BL/6J mice, and Favine KO mice were used for these experiments. We used male mice for the western diet study, carotid artery ligation study, and Favine plasma ELISA measurement and female mice for 1-year study fed with normal chow. All experimental protocols were approved by the Ethics Review Committee for Animal Experimentation of Osaka University.

Cell cultures

HUVECs were purchased from Kurabo (Japan) and cultured in MCDB 131 (Gibco) containing 10% fetal bovine serum and human fibroblast growth factor (Biovision). For the gene knockdown experiments, small interfering RNA targeting human Favine (#4427037) or nontargeting control siRNA (#4390846) was purchased from Ambion. siRNAs were transfected into HUVECs at a final concentration of 10 nM using Lipofectamine RNAiMax Transfection Reagent (Thermo Fisher Scientific). Cells were starved for 8 h in EBM-2 medium (Lonza) with 0.5% FBS and then incubated for 12 h with 10% FBS.

METHOD DETAILS

Oil Red O Stain of the aorta

Aorta of each mouse from the arch to the common iliac levels were collected. Adventitial tissues were roughly removed and aortae were fixed with 10% buffered formaldehyde and stained with Oil Red O. Each aorta was cut thoroughly vertically and laid flat on a board. The lesion area was qualified with ImageJ software (NIH). Ratios of Oil Red O positive lesion areas to total aortic wall areas were measured.

Hematoxylin and eosin staining

Tissues were fixed with 4% buffered formaldehyde, embedded in paraffin, and sectioned at a thickness of 4 μ m. The sections were stained with hematoxylin and eosin using a standard protocol as previously described (Kobayashi et al., 2015).

Measurement of cholesterol clefts

The number of cholesterol clefts normalized to total plaque numbers was counted using specimens of hematoxylin and eosin staining under microscopic observation.

von Kossa calcium stain

Aorta of each mouse from the arch to the common iliac levels was collected. Adventitial tissues were roughly removed, and aortae were fixed with 10% buffered formaldehyde and embedded paraffin and stained with calcium staining kit (Scy Tek Laboratories) according to the manufacturer's instructions. Morphological quantification of the aortic calcification was carried out using a modified method (Angulo et al., 2011). For imaging, an all-in-one fluorescence microscope (BZ-X700, KEYENCE) equipped with an advanced observation module (BZ-H3XD) and the image stitching function in the BZ-X Analyzer software (BZ-H3A) was used for image stitching. Ratios of calcified regions to aortic wall areas were measured.

Real-time RT-PCR analysis

Real-time RT-PCR was performed as previously described (JBC2015). Cells were harvested in reagent (TRI Reagent, Sigma-Aldrich) and the total RNA was isolated according to the manufacturer's instructions. cDNA was synthesized from 400 ng total RNA using an oligo (dT) 18-mer as a primer using PrimeScript Master Mix (Takara). Real-time RT-PCR was performed on Light Cycler Real-Time PCR instrument (Roche) using Fast Start Essential DNA Green Master (Roche). The primers used are listed in Table 4.

RNA-seq analysis

The bulk RNA-seq analysis of the aortas of ApoE KO mice and DKO mice fed normal chow for 1 year was carried out. RNA-seq data processing- Library preparation was performed using a TruSeq Stranded mRNA Sample Prep Kit (Illumina) according to the manufacturer's instructions. Whole-transcriptome sequencing was applied to the RNA samples with the use of an Illumina HiSeq 2500 platform in a 75-base single-end mode. Illumina CASAVA version 1.8.2 software was used for base calling. Sequenced reads were mapped to the human reference genome sequences (hg19) using TopHat version 2.0.13 in combination with Bowtie2 version 2.2.3 and SAMtools version 0.1.19. Normalized FPKM were calculated using Cuffnorm and values equal to 0.1 or less were excluded. FPKM values were logarithmically transformed (log₂) and Student's t-test was used to test the difference in the mean between WT and KO groups and to obtain p values. Genes with p values less than 0.05 were considered differentially expressed between the two groups. Geometric means of each group were calculated using FPKM values before the logarithmic transformation and fold change was calculated as the ratio of these means. The raw data obtained in this study was submitted under Gene Expression Omnibus (GEO) accession number GEO DataSets: GSE183376.

Measurements of the parameters in the blood—Blood samples were collected from the inferior vena cava veins or tail veins. Plasma glucose, triglyceride, total cholesterol, insulin, calcium, phosphate, and PAI-1 concentrations were measured using the glucose CII-test kit, triglyceride E-test (Wako Pure Chemical Industries, Tokyo, Japan), T-CHO E-test (Wako Pure Chemical Industries, Tokyo, Japan), insulin enzyme-linked immunoassay kit (Morinaga, Yokohama, Japan), calcium E-test (Wako Pure Chemical Industries, Tokyo, Japan) L type Wako IP (Wako Pure Chemical Industries, Tokyo, Japan) and PAI-1 (Molecular Innovations), respectively, according to the manufacturers' instructions.

Carotid artery ligation

At 9 weeks of age, a small midline incision was made in the neck of a male ApoE-KO, Favine/ApoE-DKO mouse fed normal chow, and the left common carotid artery was completely ligated with a 6–0 silk thread just proximal to the carotid bifurcation to disrupt the blood flow. Two weeks after the carotid ligation, the left (ligated side) and right (sham operation side) common carotid arteries were excised and analyzed. Arteries were fixed with 4% buffered formaldehyde and embedded in paraffin. Samples at 800 μm proximal to the surgical site were sectioned at a thickness of 2 μm and mounted on glass slides. Sections were stained with hematoxylin and eosin.

Analysis of Human Favine/CCDC3 expression

The Genotype-Tissue Expression (GTEx) Project was supported by the Common Fund of the Office of the Director of the National Institutes of Health, and by NCI, NHGRI, NHLBI, NIDA, NIMH, and NINDS. The data used for the analyses described in this manuscript were obtained from: dbGaP Accession phs000424.v8.p2. The data discussed in this manuscript have been deposited in NCBI's Gene Expression Omnibus (Edgar et al., 2002) and are accessible through GEO Series accession number GEO DataSets: GSE43292 (Ayari and Bricca, 2013), GEO DataSets: GSE28829 (Döring et al., 2012), and GEO DataSets: GSE120521 (Mahmoud et al., 2019).

Measurement of murine Favine concentration

We developed two monoclonal IgG antibodies against recombinant human Favine purified from human Favine- overexpressing CHO cells in immunized Favine knockout mice. We established a sandwich enzyme-linked immunosorbent assay (ELISA) system for the quantitation of Favine using these monoclonal antibodies. A standard curve was linear (Figure S9). The ELISA Kit is not commercially available currently. Blood samples were collected from the submandibular vein of C57/BL6J male mice and Favine KO male mice at the age of 9 weeks under ad-lib.

QUANTIFICATION AND STATISTICAL ANALYSIS

Statistics

The data are expressed as the mean \pm SEM. Differences between the two groups were examined for statistical significance using Student's *t*-test or the Mann–Whitney U test. A *p* value of less than 0.05 was considered statistically significant.